Triple-Dearomative Photocycloaddition – A Strategy to Construct Novel Caged Molecular Frameworks

Kaijie Ji,[1] Jayachandran Parthiban,[2] Steffen Jockusch,[2] Jayaraman Sivaguru,[2*] and John A. Porco, Jr.[1*]

[1] *Department of Chemistry and Center for Molecular Discovery (BU-CMD), Boston University, Boston, Massachusetts, 02215, United States*

[2] *Department of Chemistry and Center for Photochemical Sciences, Bowling Green State University, Bowling Green, Ohio, 43403, United States*

ABSTRACT: An unprecedented, caged *2H*-benzo-dioxo-pentacycloundecane (BDPC) framework was serendipitously obtained in a single transformation *via* a triple-dearomative photocycloaddition of chromone esters with furans. This caged structure was generated during the course of an effort to access a tricyclic, oxygen-bridged intermediate enroute to the dihydroxanthone natural product nidulalin A. Reaction scope and limitations were thoroughly investigated, revealing the ability to access a multitude of synthetically challenging caged scaffolds in a two-step sequence. Photophysical studies provided key mechanistic insights on the process for formation of the novel caged scaffold.

INTRODUCTION

Nidulalin A **1**[1] and nidulaxanthone A **2**[2] (**Figure 1**) belong to the dihydroxanthone natural product family. We have recently reported total syntheses of **1** and **2** involving use of allyl triflate for chromone ester activation followed by vinylogous addition to access the nidulalin A scaffold in a four-step sequence which also employs ketone desaturation using Bobbitt's oxoammonium salt.[3] An initial approach to target monomer **1** involved use of chromone ester **3** as a substrate for Diels-Alder cycloaddition with furan to produce the intended cycloadduct **4** (**Figure 2**) followed by base-mediated carbon-oxygen bond cleavage to dienone **5** and subsequent demethylation. Herein, we report studies on the photochemical reactivity of chromone ester substrates such as **3** with furans which led to the serendipitous discovery of a novel, triple-dearomative photocycloaddition to produce an underdeveloped, caged scaffold architecture.

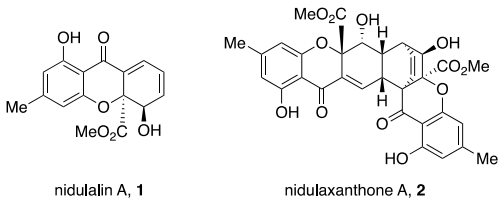

Figure 1. Dihydroxanthone natural products.

RESULTS AND DISCUSSION

After unsuccessful trials with thermal cycloaddition of chromone ester **3** with furan, we envisioned that photochemical cycloaddition from the triplet state of chromone ester **3**[4] may be employed to initiate the planned synthetic sequence illustrated in **Figure 2**. Interestingly, employing a 370 nm LED as light source and 4:1 MeCN/furan as a mixed solvent system (0.025 M), we unexpectedly obtained the novel caged compound **6** as the exclusive product with no evidence of Diels-Alder cycloadducts or *syn*-, *anti*-[2+2]-cycloaddition products (**Table 1**, entry 1). Compound **6** contains the dioxo-pentacycloundecane caged-scaffold which to the best of our knowledge has a single precedent in the literature[5] from the work of West and coworkers as a minor product (**7**, 5% yield) (**Figure 3A**). The reaction pathway from **3** and furan to **6**, an intermolecular triple-dearomative cycloaddition,[6] is unprecedented in the literature.

Polycyclic caged compounds have been widely used in medicinal chemistry[7–15] and their intriguing structures often present challenges from a synthetic chemistry standpoint[8,11,12,14,16,17] (**Figure 3B**). For example, cubane **8** is a monoamine oxidase B (MAO-B) inhibitor[18] and requires a 15-step synthesis;[8] NGP1-01 **9**[12] is a pentacycloundecane derivative with broad bioactivity[7–11,13,14,16] and requires a five-step synthesis; tromantadine **10**[19] is an adamantane derivative with antiviral activity and is synthesized in five steps. In comparison, caged compound **6** bearing the *2H*-benzo-dioxo-pentacycloundecane

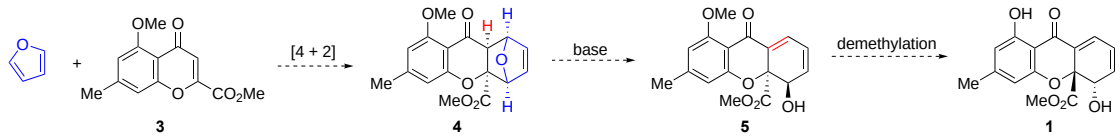

Figure 2. Original synthetic plan for the synthesis of nidulalin A *via* cycloaddition of a chromone ester and furan.

https://doi.org/10.26434/chemrxiv-2024-150z3 **ORCID:** https://orcid.org/0000-0003-2625-1791

Table 1. Discovery of caged compound 6 and reaction optimization using batch conditions. [a]

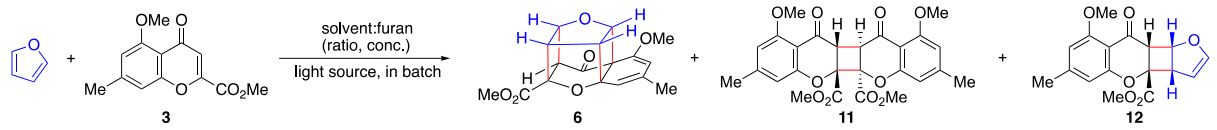

entry	light source [b]	Solvent [c]	ratio	Conc. (M)	Irradiation time (h)	Conv.(%) [d]	Ratio of **6** : **11** : **12** : **3**
1	370 nm	MeCN	4:1	0.025	20	100	100: 0 : 0 : 0
2	370 nm	MeCN	4:1	0.050	20	100	97 : 3 : 0 : 0
3	370 nm	MeCN	4:1	0.100	20	100	80 : 20 : 0 : 0
4	370 nm	toluene	4:1	0.025	24	62	35 : 17 : 0 : 48
5	370 nm	TFE	4:1	0.025	24	0	0 : 0 : 0 :100
6	390 nm	MeCN	4:1	0.025	20	65	65 : 0 : 0 : 35
7 [e]	427 nm	MeCN	4:1	0.025	24	27	0 : 0 : 27 : 73

[a] Reaction conducted on a 0.05 mmol scale. [b] Kessil lamps were employed in all cases. [c] Solvents (MeCN, toluene or TFE) and furan were degassed for 20 min before use. [d] Conversion and products ratio based on crude ^{1}H NMR analysis in neutralized $CDCl_3$. In all cases, only **6**, **11**, **12**, and **3** were observed. Neutralized $CDCl_3$ was prepared *via* passing through a short basic alumina column. [e] 5 mol% of thioxanthone included as additive.

(BDPC) moiety is synthesized in a one-step process from a chromone ester substrate and was found to be the only product in the reaction (**Figure 3A**).

In terms of reaction development, conducting reactions at a higher concentration in MeCN (**Table 1**, entries 2 & 3), in the non-polar solvent toluene (**Table 1**, entry 4), or switching the light source to a mercury lamp (λ = 254 nm) only resulted in the production of the chromone homodimer **11**.[20] Use of the protic solvent trifluoroethanol (TFE) totally mitigated reactivity and led to recovered chromone ester **3** (**Table 1**, entry 5). Switching the light source from a 370 to 390 nm LED light source resulted in slower reactions (**Table 1**, entry 6). Employing the triplet photosensitizer thioxanthone (TX) using 427 nm photoirradiation instead resulted in the production of the chromone-furan [2+2]-*syn* adduct **12** (**Table 1**, entry 7). In order to increase light penetration and further improve conversion on a larger scale, we employed a flow photoreactor setup I[21] which vastly improved reaction efficiency and delivered the caged product **6** in 95% conversion within 3 h on a 75 mg reaction-scale (**Table 2**,

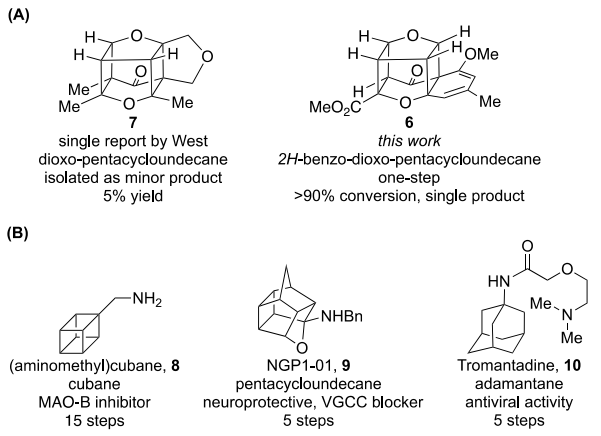

Figure 3. (A) Structural comparison of a precedented caged compound *vs.* BDPC **6**. (B) Select bioactive caged scaffolds in medicinal chemistry.

Table 2. Reaction optimization in flow to access caged compound **6**.

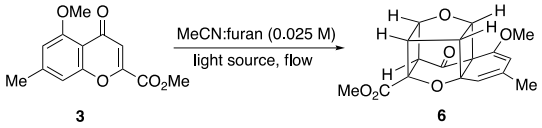

Entry	Reaction setup	Ratio of MeCN:furan[a]	Residence time (h)	Conv. (%)[b]
1 [c]	Batch	4:1	70	67
2 [d]	Setup I	4:1	3	95
3 [d]	Setup I	4:1	3	70
4 [e]	Setup II	12:1	2	81
5 [e]	Setup II	7:1	1	62
6 [e]	Setup II	7:1	2.5	92

[a] MeCN and furan were degassed for 20 min before use. [b] Conversion based on crude ^{1}H NMR analysis in neutralized $CDCl_3$. In all cases, only **3** and **6** were observed. $CDCl_3$ was neutralized by passing directly through a short basic Al_2O_3 column. [c] 50 mg scale, batch setup using a 370 nm Kessil lamp. [d] 75 mg scale, Flow photoreactor setup I.[21] [e] 100 mg scale, Flow photoreactor setup II.[21]

entry 1) which compares to a 67% conversion using batch conditions over 70 h on a 50 mg reaction scale (**Table 2**, entry 1). Further optimization using a 365 nm LED light source with a lower loading of furan (7:1 MeCN/furan) using the flow photoreactor setup II developed by Beeler and coworkers[21,22] led to a 92% conversion of **3** to **6** in 2.5 h residence time on a 100 mg reaction-scale (**Table 2**, entry 6).

Due to the instability of caged compound **6** in acidic environments which ultimately led to *retro*-[2+2]-[2+2] to chromone ester **3**, we further functionalized scaffold **6** in order to stabilize the structure **(Figure 4)**. We found that exposure of **6** to silica

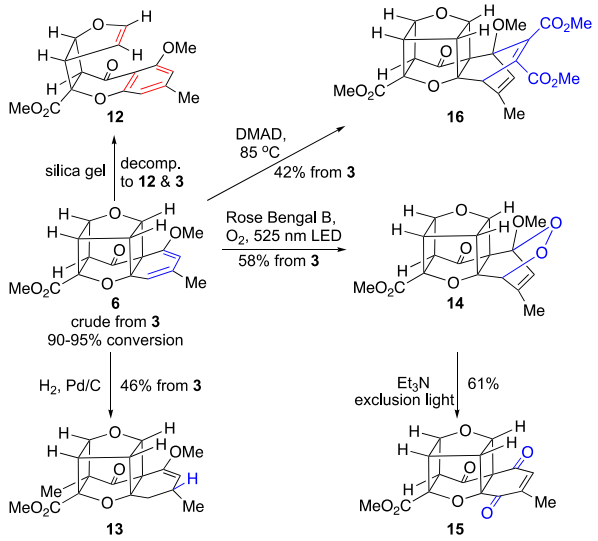

Figure 4. Production of a novel caged compound and further functionalization chemistry.

gel afforded the *retro*-[2+2] cycloadduct **12** along with chromone ester **3** as an inseparable mixture, thereby reinforcing the lability of the caged scaffold with its adjacent dienol ether moiety. Hydrogenation of **6** (Pd/C, H_2) afforded the methyl enol ether **13** in 46% yield from **3** as a stable compound. Treatment of **6** under singlet oxygen conditions (Rose Bengal B, O_2, green LED) led to the endoperoxide **14** which was isolated as a stable, tan solid in 58% yield from **3.** The intriguing hydrogenated 2,7-dioxa-1,2b-methanobenzo[1,4]cyclobuta[1,2,3-*cd*]cyclobuta[*gh*]pentalene framework of **14** was unambiguously confirmed by single X-ray crystallographic analysis (**Figure 5**). Kornblum-DeLaMare rearrangement[23] of **14** employing triethylamine (Et_3N) as base with exclusion of light led to clean conversion of **14** to enedione **15** in 61% yield. Finally, Diels-

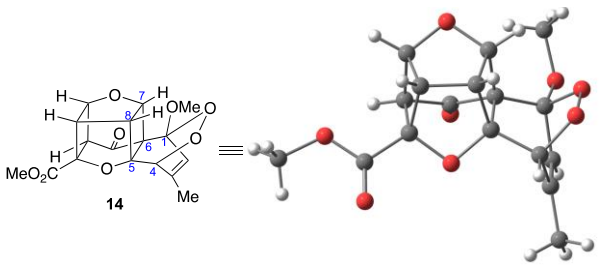

Figure 5. X-ray crystal structure of **14**.

Alder cycloaddition of **6** with dimethyl acetylenedicarboxylate (DMAD) afforded diester **16** in 42% yield (**Figure 4**). It should be noted that DMAD and singlet oxygen were sufficiently small in size to react with the congested dienol ether moiety of **6** in comparison to other dienophiles evaluated (*e.g.* maleic anhydride and benzoquinone). Moreover, Diels-Alder cycloaddition exclusively took place from the top face of caged compound **6** adjacent to the "ledge" provided by the diene and the adjacent cyclobutane ring. Based on examination of product structures, the excellent stereoselectivity for reactions affording products such as **14** and **16** may also be explained in part by the Cieplak effect[24,25] wherein the forming σ bonds participate in hyperconjugative stabilization with the C_6-C=O and C_5-O σ* orbitals of substrate **6**.

With optimized conditions in hand, we next explored the substrate scope of heterocyclic reaction partners using optimized batch or flow conditions (**Table 3**, *vide infra*). All furan substrates including 2-substituted and 2,5-disubstituted furans **17** – **20** participated as reaction partners to afford the corresponding caged compounds (*not shown*), with lower conversions observed upon increasing steric hindrance (entries 1-4). The caged compounds obtained were further functionalized to the stable derivatives **21** – **24** & **26** – **27** using previous developed conditions (*cf.* **Figure 4)**. Use of 2-methylfuran **17** as reaction partner afforded a 1:1 mixture of isomeric enol ethers **21** and **22** (34% yield, inseparable) after hydrogenation (**Table 3**, entry 1). The corresponding caged compound from **3** and 2,5-dimethylfuran **18** afforded the *retro*-[2+2] cycloadduct **23** in 49% yield after exposure to silica (**Table 3**, entry 2) and methyl enol ether **24** in 27% yield after hydrogenation (**Table 3**, entry 3). The caged compound **25** derived from 2-trimethylsilyl furan **19** was found to be very labile under mild acidic conditions and readily afforded the *retro*-[2+2] cycloadduct **26** in 49% yield by treatment in $CDCl_3$ (50 °C) (**Table 3**, entry 4). 2-Trimethylsilyl-5-methylfuran **20** afforded the corresponded caged compound as single regioisomer, likely due to the steric hindrance and blocking effect of the trimethylsilyl (TMS) group.[26] Similar to the production of **26** from **25**, cyclobutene-opening product **27** was isolated in 35% yield after treatment with $CDCl_3$ (50 °C) (**Table 3**, entry 5).

Mechanistically, we believe that cyclobutane edge protonation[27,28] in the presence of adventitious D-Cl may open the cyclobutane ring of **25** to a transient cation **28** which is stabilized by the silicon *β*-effect[29,30] followed by elimination and aromatization to afford product **26** (**Figure 6B**). Originally, we considered that **26** may be converted back to **25** *via* dearomative [2+2]-cycloaddition as DFT computational analysis (r^2SCAN-3C/CPCM (CH_2Cl_2)) of **26** showed a close distance between the corresponded alkene and the two carbons of the arene (**Figure 6C**). However, all attempts including photoirradiation **26** using a 365 nm LED or a white LED in MeCN or thermolysis failed to deliver **25** but instead led to recovery of starting material which indicated an irreversible process for formation of **26** (**Figure 6A**).

We also found that *N*-(methoxycarbonyl)pyrrole **29** could serve as reaction partner with **3** to afford the corresponded caged nitrogen-containing scaffold in lower conversion with elongated reaction time (53% conversion, 78 h in batch). Fortunately, the corresponding endoperoxide **30** from this caged intermediate could be isolated in 27% yield (*vide supra*, **Table 3**, entry 6). Unfortunately, thiophene substrates and electron-rich, *N*-substituted pyrroles such as *N*-methyl and *N*-trimethylsilyl pyrrole failed to deliver related caged compounds under similar conditions (**Table S5**).[21]

Table 3. Heterocycles substrate scope

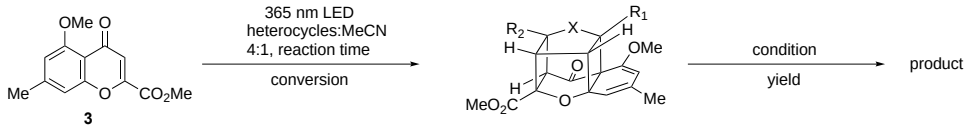

Entry	Heterocycle	Batch/flow [a]	Reaction time (h)	Conv.(%) [b]	Condition [c]	Product	Yield (%) [d]
1	 **17**	batch	42	100	A	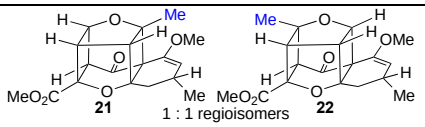 **21** 1 : 1 regioisomers **22**	34
2	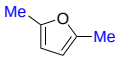 **18**	flow	2.5	77	B	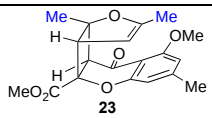 **23**	49
3		batch	46	95	A	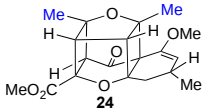 **24**	27
4	 **19**	flow	6	67	C	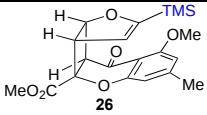 **26**	49
5	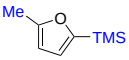 **20**	batch	44	90	C	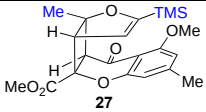 **27**	35
6	 **29**	batch	78	53	D	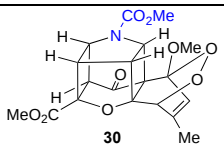 **30**	27

[a] Flow conditions employing 0.4 mmol of **3**; batch conditions employing 0.1 mmol of **3**. [b] Conversion measured by the crude ^{1}H NMR from the initial photochemical reaction with chromone ester **3**. [c] Condition A. 2 mol% Pd/C, H_2, EtOAc. Condition B. Silica gel. Condition C. $CDCl_3$, 50 °C, 36 h. Condition D. 5 mol% Rose Bengal B, O_2, $CDCl_3$/CD_3OD=9:1, 525 nm LED. [d] Yield over two steps from chromone ester **3**.

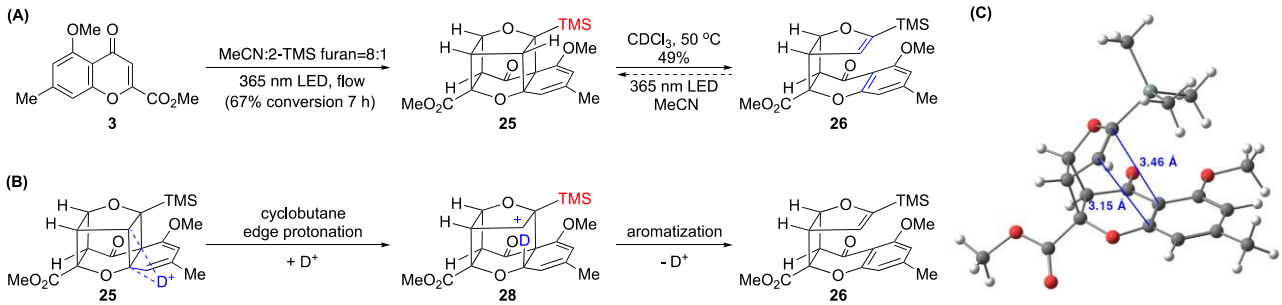

Figure 6. (A) Irreversible retro-[2+2]-cycloadduct **26** formation facilitated by cyclobutane edge protonation. (B) Proposed mechanism for formation of **26**. (C) DFT structure of compound **26** (r^2SCAN-3C/CPCM (CH_2Cl_2)).

We next explored substrate scope using various chromone substrates **31** - **35** (**Table 4**) which involved processing of the corresponding crude, caged products using conditions developed in **Figure 4**. Switching the methyl group of chromone **3** into a hydrogen (**31**) or a methoxy group (**32**) did not interfere with the formation of caged products. Accordingly, endoperoxide **36** was generated in 45% yield from **31** using flow conditions followed by endoperoxidation (**Table 4**, entry 1). We also

Table 4. Chromone substrate scope. [a]

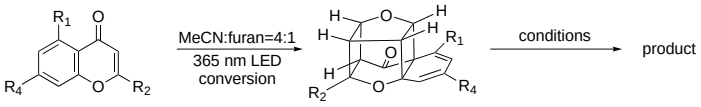

Entry	Chromone substrate	Batch/ flow	Reaction time (h)	Conv. (%) [b]	Condition [c]	Product	Yield (%) [d]
1	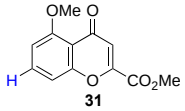 **31**	flow	2.5	91	A	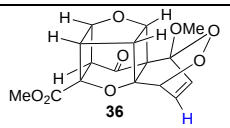 **36**	45
2	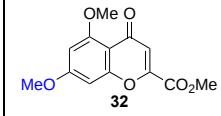 **32**	batch	67	88	B	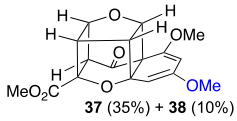 **37** (35%) + **38** (10%)	45
3					C	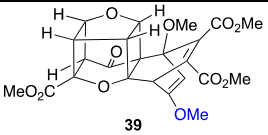 **39**	54
4			45	80	A	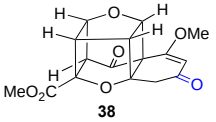 **38**	23
5	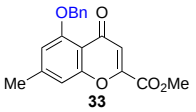 **33**	batch	24	67	A	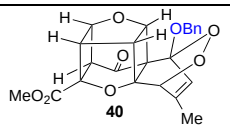 **40**	36
6	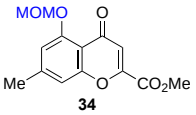 **34**	batch	44	75	A	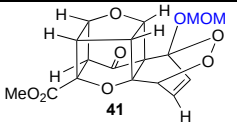 **41**	47
7	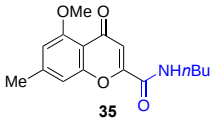 **35**	batch	47	67	D	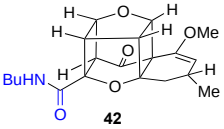 **42**	50

[a] Flow conditions employing 0.4 mmol of chromone substrate; batch conditions employing 0.1 mmol of chromone substrate. [b] conversion measured by crude ^{1}H NMR analysis from the initial photochemical reaction with furan. [c] Condition A. 5 mol% Rose Bengal B, O_2, $CDCl_3/CD_3OD$=9:1, 525 nm LED. Condition B. Silica gel. Condition C. 10 equiv. DMAD, toluene, 85 ^oC. Condition D. 2 mol% Pd/C, H_2, EtOAc. [d] Yield over two steps from chromone ester.

found that diene **37** from dimethoxy chromone ester substrate **32** was a relatively stable caged product on silica gel and could be isolated in 35% yield together with 10% of the hydrolyzed methoxy enone **38** produced by acid hydrolysis on silica gel (**Table 4**, entry 2). Thermolysis of **37** with DMAD afforded the cycloadduct **39** in 54% yield (**Table 4**, entry 3). Interestingly, the hydrolysis product 3-methoxy cyclohex-2-enone **38** was isolated as the exclusive product in 23% yield from crude **37** using Rose Bengal B/O_2 conditions; we did not observe the expected endoperoxide as in other cases (**Table 4**, entry 4). Rose Bengal-catalyzed demethylation and photocatalytic hydrolysis of enol ethers have been reported in the literature.[31,32] Switching the *peri*-methoxy group of **3** into a *peri*-benzyloxy (**33**) or a *peri*-methoxymethyl group (**34**) led to similar results in comparison to substrate **3** affording endoperoxides **40** and **41** in 36% and 47% yields, respectively, using batch conditions followed by endoperoxidation (**Table 4**, entries 5 & 6). Switching the ester moiety of **3** into an amide (**35**) resulted in similar reactivity; the corresponding caged compound was further reduced to enol ether **42** in 50% yield using Pd/C/H_2 (**Table 4**, entry 7).

To gain additional insight into the formation of caged compound **6** and its derivatives, we performed a detailed photophysical investigation using the key reaction partner **3**. Chromone ester **3** absorbs light below ~390 nm and shows two peaks at 325 nm and 274 nm with molar absorptivities of 6728 and 18117 $M^{-1}cm^{-1}$, respectively (**Figure 7A**, blue line). Addition of furan to solutions of **3** did not cause significant changes in

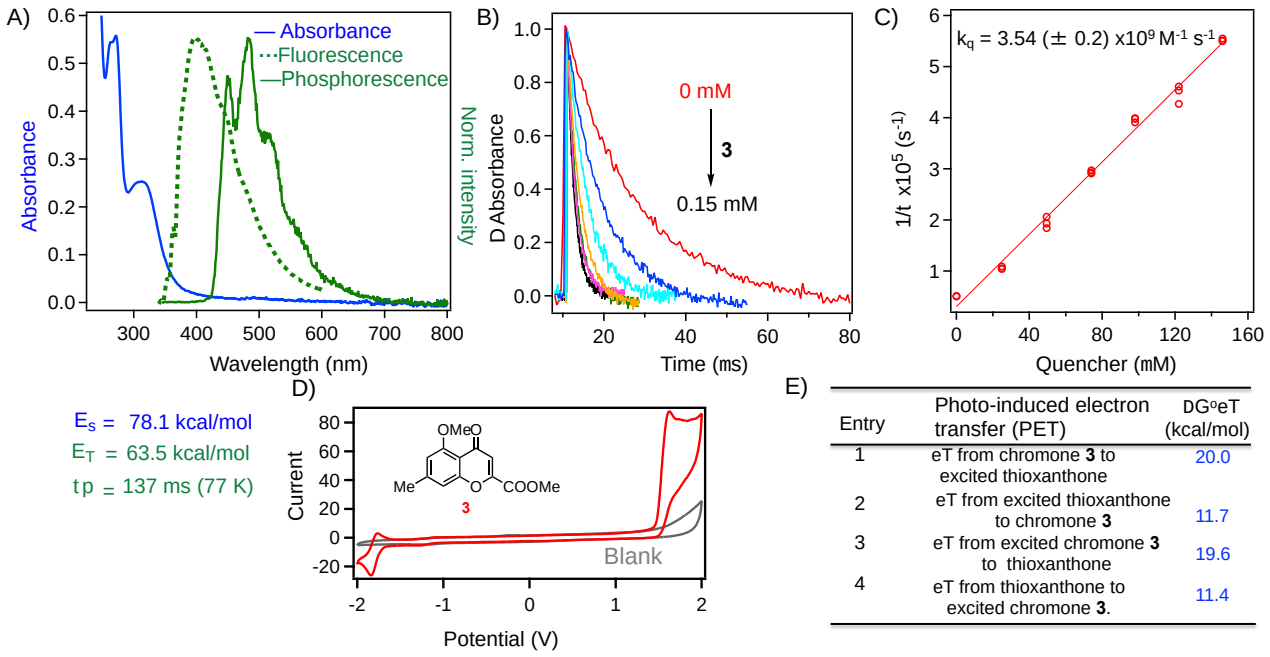

Entry	Photo-induced electron transfer (PET)	DG°eT (kcal/mol)
1	eT from chromone **3** to excited thioxanthone	20.0
2	eT from excited thioxanthone to chromone **3**	11.7
3	eT from excited chromone **3** to thioxanthone	19.6
4	eT from thioxanthone to excited chromone **3**.	11.4

Figure 7. (A) UV-Vis absorption spectrum in EtOH at rt (blue); fluorescence spectrum in EtOH (λ_{ex} = 325 nm) at rt (dotted; green); time-resolved phosphorescence spectrum recorded 5–55 ms after pulsed excitation at 325 nm in EtOH glass at 77 K (solid; green). (B) Thioxanthone triplet decay traces (Δ absorbance) monitored at 620 nm measured by laser flash photolysis (λ_{ex} = 355 nm, 7 ns pulse width) in the absence and presence of different concentrations of **3** in argon saturated CH_3CN solutions. (C) Determination of the bimolecular quenching rate constant k_q of quenching of thioxanthone triplet states by **3** using the kinetic data shown in (B). Plot of the inverse triplet lifetime *vs.* concentration of **3**. (D) CV experiment for **3**. (E) Free energy for electron transfer under sensitized conditions.

absorbance above 300 nm indicating that no ground state EDA complexes[33] are formed between **3** and furan.[21] Having ascertained that the reaction does not proceed *via* ground state EDA complex formation, the excited state properties of **3** were further investigated.[21] Photoexcitation of **3** at 330 nm generated weak fluorescence (**Figure 7A**, dotted green line). The energy of the lowest singlet excited state of **3** (78.1 kcal/mol^{-1}) was estimated from the intercept of the absorption and fluorescence spectra (**Figure S4**).[21] The low fluorescence quantum yield (<0.005), determined by comparison to the standard (9,10-diphenylanthracene),[34] indicates fast singlet excited state deactivation processes including intersystem crossing (ISC) into the triplet state. Phosphorescence studies were performed to investigate the formation and energy of triplet states. **Figure 7A** (green line) shows the phosphorescence spectrum of **3** at 77 K in an EtOH matrix and has a lifetime of 137 ms. The energy of the triplet state was determined from the highest-energy peak (63.5 kcal/mol). These point to the ππ* nature of the lowest triplet excited state. It is possible that the nπ* triplet state is close in energy to the ππ* triplet state resulting in intermixing. Such a scenario for **3** is similar to the excited state features of enone derivatives.[35] This may be a key reason why the fluorescence quantum yield was low in **3** coupled with a strong phosphorescence. As shown above, the photoreaction proceeded efficiently in the presence of TX as triplet sensitizer. We then determined the bimolecular quenching rate constant of TX triplet states by **3** using laser flash photolysis. Laser excitation (λ_{ex} = 355 nm, pulse width = 7 ns) of an argon-saturated solution of TX in acetonitrile generated a triplet transient absorption centered at ~620 nm[37] which was quenched by **3** (**Figure 7B**). The bimolecular quenching rate constant was determined from the slope of the plot of the inverse triplet lifetimes *vs.* the concentration of **3** which gave a close to diffusion-controlled rate constant (k_q = 3.54 (± 0.2) × 10^9 M^{-1} s^{-1}; **Figure 7C**). The quenching of triplet excited states by **3** may proceed by energy or electron transfer. As the triplet energy of the sensitizer thioxanthone **43** (TX = 64 kcal/mol)[37] and the chromone (**3** = 63.5 kcal/mol) are close,[21] one can anticipate energy transfer from the sensitizer to the chromone ester substrate. By using the Rehm–Weller equation, we also evaluated the viability of photoinduced electron transfer (PET) playing a role under sensitized conditions. Inspection of the Table (**Figure 7E**) revealed an endergonic electron transfer from excited sensitizer **43** (^{3}TX*) to chromone **3** as well as triplet excited chromone (^{3}**3***) to sensitizer **43** (TX). Due to the highly endergonic nature of electron transfer in the reaction of TX triplets with **3** and the close to diffusion-controlled rate constant of ^{3}TX* quenching by **3**, energy transfer is the most likely pathway for the reaction generating triplet-excited states of **3**. In addition, the photoexcited oxidative potential of **3** was calculated to be –1.13 eV by use of the Rehm-Weller approximation which is insufficient to oxidize furan (E_{ox} = +1.80 eV). As was previously mentioned, *N*-methyl pyrrole (E_{ox} = +1.09 eV) with feasible oxidative potential by the photoexcited state of **3**, failed to deliver the corresponding caged compound with **3** but rather returned starting material. As a result, only the triplet excited state of substrate **3** appears to be involved in the formation of caged scaffold **6.**

As we established the formation of triplet excited state of **3** upon direct irradiation through photophysical studies, we propose a mechanism for the formation of the caged photoproduct **6** (**Figure 8**). As a working hypothesis, we believe that the triplet excited chromone ^{3}[**3**]* is generated upon direct irradiation of **3**. This is reasonable as we observed a very weak fluorescence of **3** with low quantum yields. The triplet-excited

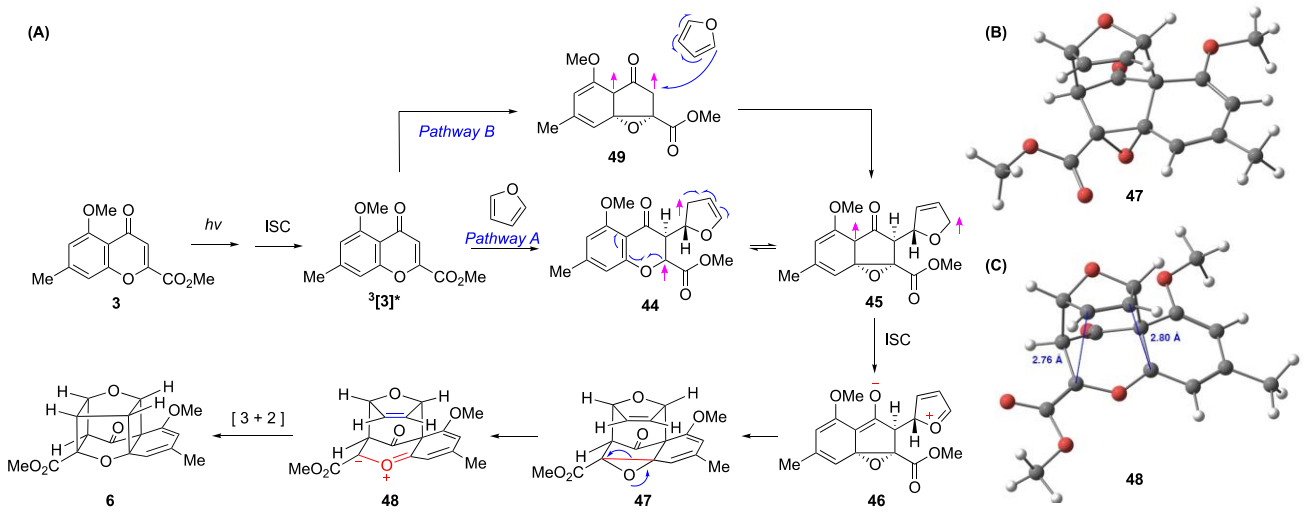

Figure 8. (A) Proposed mechanism for the formation of **6**. (B) DFT computations of oxirane **47** (r^2SCAN-3C/CPCM (CH_2Cl_2)). (C) DFT computations of carbonyl ylide **48** (r^2SCAN-3C/CPCM (CH_2Cl_2)).

chromone ^{3}[**3**]* subsequently reacts with furan to generate a triplet biradial species **44** (**Figure 8**). This triplet diradical **44** undergoes dearomative cyclization leading to **45** followed by intersystem crossing (ISC) to form the zwitterionic intermediate **46**. This intermediate **46** undergoes cyclization to **47** (**Figure 8**) which may subsequently ring-open to carbonyl ylide **48** (**Figure 8**)[38,39] followed by intramolecular (3+2) cycloaddition[38,39] to the caged cycloadduct **6** (**Figure 8**, Pathway A). An alternative mechanism (**Figure 8**, Pathway B) can be envisioned for the formation of **6** that features the tautomeric, dearomatized triplet diradical intermediate **49** generated from the triplet excited chromone ^{3}[**3**]* which is reminiscent of diradical intermediates observed and proposed in oxa-di-π-methane rearrangements of substrates including cyclohexadienones.[40] The diradical intermediate **49** may react with furan in a stepwise fashion (as it occurs in a triplet manifold) to form a triplet biradical **45**. This triplet biradical **45** intersystem crosses to the zwitterionic species **46** enroute to the formation of cycloadduct **6**. A point to note is that diradical intermediate **49** can also intersystem cross to an oxyallyl cation type species (similar to the intermediates proposed by West and co-workers)[5] followed by formal addition of furan to form intermediate **46**.

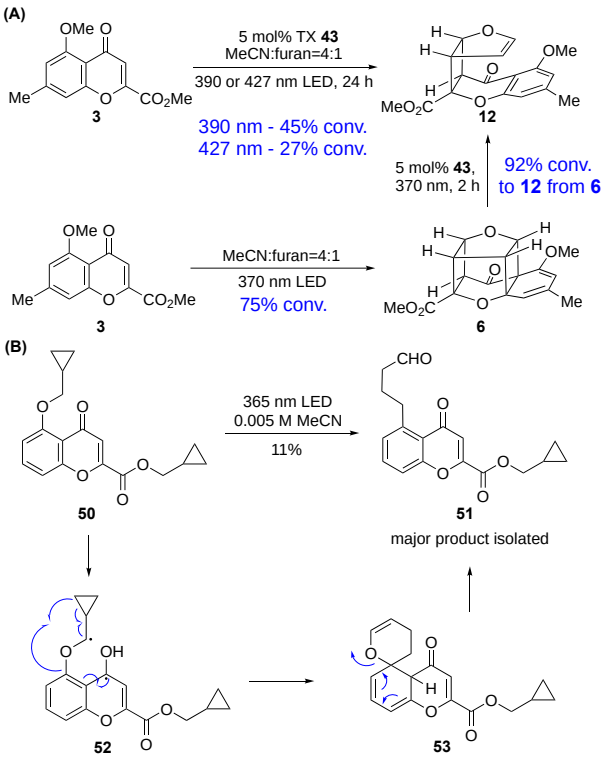

Figure 9. (A) Mechanistic studies involving thioxanthone **43**. (B) Radical clock experiment to probe HAT.

To validate and further study the proposed mechanism depicted in **Figure 8**, we carried out the series of control studies detailed in **Figure 9A/B**). In the first experiment (**Figure 9A**), we employed triplet energy transfer by utilizing thioxanthone **43** (E_T = 64 kcal/mol) as the triplet photosensitizer to generate triplet excited chromone ^{3}[**3**]* that was established to have a triplet energy of ~63.5 kcal/mol (**Figure 7A**). Sensitized irradiation of chromone **3** under energy transfer conditions with thioxanthone **47** in the presence of furan in acetonitrile as solvent (MeCN/furan = 4:1) resulted in the formation of [2+2]-photoproduct **12**. To rationalize the formation of [2+2]-photoproduct **12** under triplet sensitization, we subjected the caged photoadduct **6** to sensitized irradiation with thioxanthone **43** and were able to observe the formation of [2+2]-photoproduct **12**. This is due to the fact that **6** features a diene chromophore that likely has a triplet ππ* excited state with energy similar to that of thioxanthone **43**. Specifically, triplet-excited **6** generated upon energy transfer from thioxanthone[42] undergoes β-cleavage resulting in the formation of the [2+2]-photoproduct **12**. Alternatively, an electron transfer from the diene **6** to the excited thioxanthone followed by cleavage of the dienyl-cation resulting in the formation of the [2+2]-photoproduct **12**, cannot be ruled out. In the second of experiments (**Figure 9B**), the cyclopropyl chromone radical clock substrate **50** was subjected to direct irradiation which resulted in the formation of **51**, albeit in 11% yield. The formation of **51** can be rationalized by intramolecular H-atom abstraction from the triplet excited chromone ^{3}[**50**]* to generate diradical **52** which may be followed by spirocyclization to intermediate **53** and elimination/rearomatization. The

latter experiment once again reinforces that the triplet excited state of **3** and related chromone esters have ππ* character intermixed with the higher lying nπ* triplet excited state as observed in our photophysical studies.

CONCLUSION

In summary, we serendipitously discovered and synthesized an unprecedented caged system bearing a *2H*-benzo-dioxo-pentacycloundecane (BDPC) scaffold in a single transformation from photoirradiation of chromone esters and furans *via* triple-dearomative cycloaddition. Flow photoreactors were employed for reaction scale-up and a series of subsequent functionalizations of the caged scaffold were developed in a one-pot, two-step manner. Overall, 25 caged compounds were prepared in yields ranging from 27 – 58% encompassing variations of both chromone and heterocycle substrates. Photophysical studies provided key mechanistic insights on the process for formation of the novel caged scaffold. We believe that the novel compounds produced in this study should provide further impetus for research on the rapid synthesis of novel caged structures for use in drug discovery and medicinal chemistry. Further studies on the chemistry of the caged BDPC architecture as well as biological evaluation of the scaffolds are currently in progress and will be reported in due course.

ASSOCIATED CONTENT

Supporting Information

The Supporting Information is available free of charge at https://pubs.acs.org/doi/XXXXXX

Experimental procedures, analytical data, and ^{1}H and ^{13}C NMR spectra of all newly synthesized compounds, X-ray crystallographic analysis of compounds **14** and **39**, DFT calculation details, and photophysical studies (PDF).

AUTHOR INFORMATION

Corresponding Author

John A. Porco, Jr. − *Department of Chemistry and Center for Molecular Discovery (BU-CMD), Boston University, Boston, Massachusetts 02215, United States; orcid.org/0000-0002-2991-5680*; Email: porco@bu.edu

Jayaraman Sivaguru – *Department of Chemistry and Center for Photochemical Sciences, Bowling Green State University, Bowling Green, Ohio, 43403, United States; orcid.org/0000-0002-0446-6903*

E-mail: sivagj@bgsu.edu

Author

Kaijie Ji − *Department of Chemistry and Center for Molecular Discovery (BU-CMD), Boston University, Boston, Massachusetts 02215, United States;* orcid.org/*0000-0003-2625-1791*

Jayachandran Parthiban – *Department of Chemistry and Center for Photochemical Sciences, Bowling Green State University, Bowling Green, Ohio, 43403, United States; orcid.org/0000-0002-5916-1701*

Steffen Jockusch – *Department of Chemistry, Bowling Green State University, Bowling Green, Ohio, 43403, United States; orcid.org/0000-0002-4592-5280*

Funding Sources

R35 GM 118173 (NIH)

CHE-1955524 (NSF)

Notes

The authors declare no competing financial interest.

ACKNOWLEDGMENTS

K.J. and J.A.P, Jr. thank the National Institutes of Health (NIH) (R35 GM 118173 for financial support. We thank Dr. Jeffrey Bacon (Boston University) for assistance with X-ray crystal structure analysis, Professor Aaron Beeler and Dr. Matthew Mailloux (Boston University) for help with flow photoreactor construction and use. We thank the National Science Foundation (NSF) for support and Professor Joseph Derosa (Boston University) for helpful discussions. NMR (CHE-0619339) and MS (CHE-0443618) facilities at BU and the NIH (S10OD028585) for support of the single-crystal XRD system. Computational work at Boston University reported in this paper was performed on the Shared Computing Cluster (SCC) which is administered by Boston University's Research Computing Services. J.S. thanks the National Science Foundation for generous support for his research program (CHE-1955524) and for the purchase of excitation sources used in the photophysical experiments. J.P. thanks the Center for Photochemical Sciences for a Taller Fellowship.

REFERENCES

(1) Kawahara, N.; Sekita, S.; Satake, M.; Udagava, S.; Kawai, K. Structures of a New Dihydroxanthone Derivative, Nidulalin A, and a New Benzophenone Derivative, Nidulalin B, from *Emericella Nidulans*. *Chem. Pharm. Bull (Tokyo)*, **1994**, *42* (9), 1720–1723.

(2) Wang, F.; Jiang, J.; Hu, S.; Hao, X.; Cai, Y.; Ye, Y.; Ma, H.; Sun, W.; Cheng, L.; Huang, C.; Zhu, H.; Zhang, H.; Zhang, G.; Zhang, Y. Nidulaxanthone A, a Xanthone Dimer with a Heptacyclic 6/6/6/6/6/6/6 Ring System from Aspergillus Sp.-F029. *Org. Chem. Front.* **2020**, *7* (7), 953–959.

(3) Ji, K.; Johnson, P. R.; McNeely, J.; Faruk, M. Al; Porco, A. J. J. Asymmetric Synthesis of Nidulalin A and Nidulaxanthone A: Selective Carbonyl Desaturation Using an Oxoammonium Salt. *J. Am. Chem. Soc.* **2024**, *146* (7), 4892–4902.

(4) Sakamoto, M.; Yagishita, F.; Kanehiro, M.; Kasashima, Y.; Mino, T.; Fujita, T. Exclusive Photodimerization Reactions of Chromone-2-Carboxylic Esters Depending on Reaction Media. *Org. Lett* **2010**, *12* (20), 4435–4437.

(5) West, F. G.; Hartke-Karger, C.; Koch, D. J.; Kuehn, C. E.; Arif, A. M. Intramolecular [4 + 3]-Cycloadditions of Photochemically Generated Oxyallyl Zwitterions: A Route to Functionalized Cyclooctanoid Skeletons. *J. Org. Chem.* **1993**, *58* (24), 6795–6803.

(6) For examples of double-dearomative cycloadditions, see: (a) Zhu, M.; Xu, H.; Zhang, X.; Zheng, C.; You, S.-L. Visible-Light-Induced Intramolecular Double Dearomative Cycloaddition of Arenes. *Angew. Chem. Int. Ed.* **2021**, *60* (13), 7036–7040. (b) Zhen, G.; Zeng, G.; Jiang, K.; Wang, F.; Cao, X.; Yin, B. Visible-Light-Induced Diradical-Mediated Ipso-Cyclization towards Double Dearomative [2+2]-Cycloaddition or Smiles-Type Rearrangement. *Chem. Eur. J.* **2023**, *29* (15), e202203217.

(7) Van der Schyf, C. J.; Geldenhuys, W. J. Polycyclic Compounds: Ideal Drug Scaffolds for the Design of Multiple Mechanism Drugs? *Neurotherapeutics.* **2009**, *6* (1), 175–186.

(8) Young, L.-M.; Geldenhuys, W. J.; Domingo, O. C.; Malan, S. F.; Van der Schyf, C. J. Synthesis and Biological Evaluation of Pentacycloundecylamines and Triquinylamines as Voltage-Gated Calcium Channel Blockers. *Arch. Pharm (Weinheim)*. **2016**, *349* (4), 252–267.

(9) Beinat, C.; Banister, S. D.; Hoban, J.; Tsanaktsidis, J.; Metaxas, A.; Windhorst, A. D.; Kassiou, M. Structure–Activity Relationships of N-Substituted 4-(Trifluoromethoxy)Benzamidines with Affinity for GluN2B-Containing NMDA Receptors. *Bioorg Med Chem. Lett.* **2014**, *24* (3), 828–830.

(10) Zindo, F. T.; Barber, Q. R.; Joubert, J.; Bergh, J. J.; Petzer, J. P.; Malan, S. F. Polycyclic Propargylamine and Acetylene Derivatives as Multifunctional Neuroprotective Agents. *Eur. J. Med. Chem.* **2014**, *80*, 122–134.

(11) Zindo, F. T.; Malan, S. F.; Omoruyi, S. I.; Enogieru, A. B.; Ekpo, O. E.; Joubert, J. Design, Synthesis and Evaluation of Pentacycloundecane and Hexacycloundecane Propargylamine Derivatives as Multifunctional Neuroprotective Agents. *Eur. J. Med. Chem.* **2019**, *163*, 83–94.

(12) Geldenhuys, W. J.; Malan, S. F.; Murugesan, T.; Van der Schyf, C. J.; Bloomquist, J. R. Synthesis and Biological Evaluation of Pentacyclo[5.4.0.02,6.03,10.05,9]Undecane Derivatives as Potential Therapeutic Agents in Parkinson's Disease. *Bioorg. Med. Chem.* **2004**, *12* (7), 1799–1806.

(13) Joubert, J.; Geldenhuys, W. J.; Van der Schyf, C. J.; Oliver, D. W.; Kruger, H. G.; Govender, T.; Malan, S. F. Polycyclic Cage Structures as Lipophilic Scaffolds for Neuroactive Drugs. *ChemMedChem* **2012**, *7* (3), 375–384. https://doi.org/https://doi.org/10.1002/cmdc.201100559.

(14) Kapp, E.; Joubert, J.; Sampson, S. L.; Warner, D. F.; Seldon, R.; Jordaan, A.; de Vos, M.; Sharma, R.; Malan, S. F. Antimycobacterial Activity, Synergism, and Mechanism of Action Evaluation of Novel Polycyclic Amines against *Mycobacterium Tuberculosis*. *Adv. Pharmacol. Pharm. Sci.* **2021**, *2021*, 5583342.

(15) Ragshaniya, A.; Kumar, V.; Tittal, R. K.; Lal, K. Nascent Pharmacological Advancement in Adamantane Derivatives. *Arch. Pharm (Weinheim).* **2023**, e2300595.

(16) James, B.; Viji, S.; Mathew, S.; Nair, M. S.; Lakshmanan, D.; Ajay Kumar, R. Synthesis of Novel Highly Functionalized Biologically Active Polycyclic Caged Amides. *Tetrahedron Lett.* **2007**, *48* (35), 6204–6208.

(17) Bliese, M.; Tsanaktsidis, J. Dimethyl Cubane-1,4-Dicarboxylate: A Practical Laboratory Scale Synthesis. *Aust. J. Chem.* **1997**, *50* (3), 189–192.

(18) Silverman, R. B.; Zhou, J. P.; Eaton, P. E. Inactivation of Monoamine Oxidase by (Aminomethyl)Cubane. First Evidence for an .alpha.-Amino Radical during Enzyme Catalysis. *J. Am. Chem. Soc.* **1993**, *115* (19), 8841–8842.

(19) Rosenthal, K. S.; Sokol, M. S.; Ingram, R. L.; Subramanian, R.; Fort, R. C. Tromantadine: Inhibitor of Early and Late Events in Herpes Simplex Virus Replication. *Antimicrob. Agents. Chemother.* **1982**, *22* (6), 1031–1036.

(20) Sakamoto, M.; Kanehiro, M.; Mino, T.; Fujita, T. Photodimerization of Chromone. *Chem. Comm.* **2009**, 17, 2379–2380.

(21) Please see the Supporting Information for complete experimental details.

(22) Lenihan, J. M.; Mailloux, M. J.; Beeler, A. B. Multigram Scale Synthesis of Piperarborenines C-E. *Org. Process. Res. Dev.* **2022**, *26* (6), 1812–1819.

(23) Kornblum, N.; DeLaMare, H. E. The Base Catalyzed Decomposition of A Dialkyl. *J. Am. Chem. Soc.* **1951**, *73* (2), 880–881.

(24) Kim, S.; Ciufolini, M. A. Complete Facial Selectivity in the Diels–Alder Reaction of a 5-Amino-5-Carboxycyclopentadiene Derivative. *Org. Lett.* **2011**, *13* (12), 3274–3277.

(25) Coxon, J. M.; McDonald, D. Q. The "Cieplak Effect": Hyperconjugative Interactions in Diels Alder Reactions. *Tetrahedron Lett.* **1992**, *33* (5), 651–654.

(26) Schreiber, S. L.; Desmaele, D.; Porco, J. A. On the Use of Unsymmetrically Substituted Furans in the Furan-Carbonyl Photocycloaddition Reaction: Synthesis of a Kadsurenone-Ginkgolide Hybrid. *Tetrahedron Lett.* **1988**, *29* (51), 6689–6692.

(27) Lee, C. C.; Ko, E. C. F. A Search for Protonated Cyclobutane. *Can. J. Chem.* **1976**, *54* (11), 1722–1725.

(28) Pakkanen, T.; Whitten, J. L. Theoretical Studies of the Protonation of Cyclobutane. *J. Am. Chem. Soc.* **1975**, *97* (22), 6337–6340.

(29) Roberts, D. D.; McLaughlin, M. G. Strategic Applications of the β-Silicon Effect. *Adv. Synth. Catal.* **2022**, *364* (14), 2307–2332.

(30) Lambert, J. B.; Zhao, Y.; Emblidge, R. W.; Salvador, L. A.; Liu, X.; So, J.-H.; Chelius, E. C. The β Effect of Silicon and Related Manifestations of σ Conjugation. *Acc. Chem. Res.* **1999**, *32* (2), 183–190.

(31) Lindner, J. H. E.; Kuhn, H. J.; Gollnick, K. Demethylierung von Codein Zu Norcodein Durch Sensibilisierte Photooxygenierung. *Tetrahedron Lett.* **1972**, *13* (17), 1705–1706.

(32) Gassman, P. G.; Bottorff, K. J. Electron Transfer Induced Desilylation of Trimethylsilyl Enol Ethers. *J. Org. Chem.* **1988**, *53* (5), 1097–1100.

(33) Crisenza, G. E. M.; Mazzarella, D.; Melchiorre, P. Synthetic Methods Driven by the Photoactivity of Electron Donor–Acceptor Complexes. *J. Am. Chem. Soc.* **2020**, *142* (12), 5461–5476.

(34) Morris, J. V; Mahaney, M. A.; Huber, J. R. Fluorescence Quantum Yield Determinations. 9,10-Diphenylanthracene as a Reference Standard in Different Solvents. *J. Phys. Chem.* **1976**, *80* (9), 969–974.

(35) For Photoexcited State of Enone, See: a) N. J. Turro, V. Ramamurthy, J. C. Scaiano, Modern Molecular Photochemistry of Organic Molecules, University Science Books, **2010**, 629 – 704. b) D. I. Schuster, G. Lem, N. A. Kaprinidis, New insights into an old mechanism: [2 + 2] photocycloaddition of enones to alkenes. *Chem. Rev.* **1993**, 93, 3 – 22. c) Vallavoju, N.; Sreenithya, A.; Ayitou, A. J. L.; Jockusch, S.; Sunoj, R. B.; Sivaguru, J. Photoreactions with a Twist: Atropisomerism-Driven Divergent Reactivity of Enones with UV and Visible Light. *Chem. Eur. J.* **2016**, *22* (32), 11339-11348.

(36) For Photophysical Data of Thioxanthone, See: (a) Ahuja, S.; Baburaj, S.; Valloli, L. K.; Rakhimov, S. A.; Manal, K.; Kushwaha, A.; Jockusch, S.; Forbes, M. D. E.; Sivaguru, J. Photochemical [2+4]-Dimerization Reaction from the Excited State. *Angew. Chem. Int. Ed.* **2023**. (b) Ahuja, S.; Raghunathan, R.; Kumarasamy, E.; Jockusch, S.; Sivaguru, J. Realizing the Photoene Reaction with Alkenes under Visible Light Irradiation and Bypassing the Favored [2 + 2]-Photocycloaddition. *J. Am. Chem. Soc.* **2018**, *140* (41), 13185-13189. (c) Kumarasamy, E.; Raghunathan, R.; Jockusch, S.; Ugrinov, A.; Sivaguru, J. Tailoring Atropisomeric Maleimides for Stereospecific [2 + 2] Photocycloaddition—Photochemical and Photophysical Investigations Leading to Visible-Light Photocatalysis. *J. Am. Chem. Soc.* **2014**, *136* (24), 8729-8737.

(37) Iyer, A.; Clay, A.; Jockusch, S.; Sivaguru, J. Evaluating Brominated Thioxanthones as Organo-Photocatalysts. *J. Phys. Org. Chem.* **2017**, *30* (9), e3738.

(38) Padwa, A. Intramolecular Cycloaddition of Carbonyl Ylides as a Strategy for Natural Product Synthesis. *Tetrahedron* **2011**, *67* (42), 8057–8072.

(39) McMills, M. C.; Wright, D. Carbonyl Ylides. In *Synthetic Applications of 1,3-Dipolar Cycloaddition Chemistry Toward Heterocycles and Natural Products*; Chemistry of Heterocyclic Compounds: A Series of Monographs; **2002**, 253–314.

(40) Bos, P. H.; Antalek, M. T.; Porco, J. A. Jr.; Stephenson, C. R. J. Tandem Dienone Photorearrangement–Cycloaddition for the Rapid Generation of Molecular Complexity. *J. Am. Chem. Soc.* **2013**, *135* (47), 17978–17982.

(41) Wang, Z.; Liu, J. All-Carbon [3 + 2] Cycloaddition in Natural Product Synthesis. *Beilstein. J. Org. Chem.* **2020**, *16*, 3015–3031.

(42) Strieth-Kalthoff, F.; James, M. J.; Teders, M.; Pitzer, L.; Glorius, F. Energy Transfer Catalysis Mediated by Visible Light: Principles, Applications, Directions. *Chem. Soc. Rev.* **2018**, *47* (19), 7190–7202.

Table of Contents

Triple-dearomative photocycloaddition

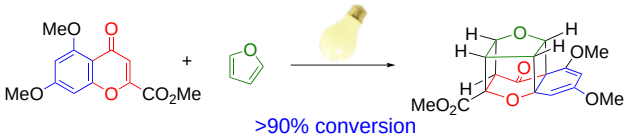

>90% conversion
single product